Tin···Oxygen Tetrel Bonding: A Combined Structural, Spectroscopic and Computational Study

Hussain Ullah,[1,2] Brendan Twamley,[1] Amir Waseem,[2] Muhammed Khawar Rauf,[2] Muhammad Nawaz Tahir, [3] James A. Platts,[4] and Robert J. Baker*[1]*

1 School of Chemistry, University of Dublin, Trinity College, Dublin 2, Ireland

2 Department of Chemistry, Quaid-i-Azam University, Islamabad-45320, Pakistan

3 Department of Physics, University of Sargodha, Sargodha, Pakistan

4 School of Chemistry, Main Building, Cardiff University, Park Place, Cardiff, CF10 3AT, U.K.

KEYWORDS: Non-covalent interactions; tin-oxygen interactions; DFT; AIM

ABSTRACT. A series of R_2Sn (R = Me, Ph) complexes of the Schiff's base salicylaldehyde acyldihydrazone with a methylene spacer of variable length have been structurally characterized in order to explore the prevalence of Sn···O non-covalent interactions. Structural studies show that these can exist, with the shortest Sn···O distance of 3.480(2) Å in this library of compounds, significantly shorter than the sum of the van der Waals radii (3.92 Å). Crystallographic studies

also show that steric effects are important and these interactions are seen only for compounds with Me_2Sn whilst they are not observed for Ph_2Sn. However this is not simply a steric effect and C—H···O interactions can compete with these Sn···O interactions. A computational study, in combination with QTAIM, shows that these interactions are mostly electrostatic in origin with little evidence of covalency.

Introduction

There are a number of types of non-covalent interactions that can be exploited to design supramolecular structures[1,2] and catalysts.[3,4] Whilst hydrogen bonding continues to be a mainstay of such interactions, there is a growing realization that halogen interactions can also be utilized. This field has been the subject of a number of recent reviews,[5,6,7,8] but what comes from experimental and theoretical studies has been the importance of the σ-hole concept.[9,10,11,12,13,14] Over the past few years other non-conventional noncovalent interactions have gained attention, such as tetrel bonding,[15,16,17,18,19] pnictogen bonding,[20,21,22,23,24,25,26,27,28,29,30,31] chalcogenide bonding,[32,33,34,35,36,37,38,39,40,41,42,43,44] and even aerogen bonding.[45] All follow the same bonding scheme, namely a σ-hole,[46] which can be viewed comparably to hydrogen bonding: X—D···A, where X is any atom, D is the donor atom and A is the acceptor atom. The σ-hole is visualized as a region of positive electrostatic potential found on an empty σ* orbital and is dependent upon two parameters: (1) the σ-hole becomes more positive (and hence forms stronger interactions) when D is more polarizable and when the X atom is more electron withdrawing. The atomic polarizability increases down the group so that for group 14: C = 11.5 au, Si = 38.1 au, Ge = 40.3 au and Sn = 55.6 au (au = atomic units);[47] thus a stronger interaction should occur when descending the group,

and there is emerging evidence that lead also participates in these interactions.[48,49,50] There are examples in the literature of experimental[51] and theoretical[52] tetrel bonding, which was only been named as such in 2013-2014. Others have described this interaction as the group 14 atom acting as a Lewis acid and the other partner in the interaction modelling an S_N2 nucleophilic attack .[53,54,55,56] Notwithstanding this, tetrel bonding is unique in that the σ-hole is located in the middle of three sp^3-hybridised bonds which means accessibility is rather low. The heavier members of this group readily participate in hyper-valency and this may lead to a strategy to ameliorate the accessibility problem.[57]

In this work we have prepared a series of Sn(IV) complexes of a Schiff's base ligand based on the salicylaldehyde acyldihydrazone core and variable length of the methylene spacer to explore the steric influences on intermolecular tetrel bonding between tin and oxygen. The structural studies have been augmented by computational methods which show that the Sn···O interactions are electrostatic in origin, but of comparable strength to the C—H···O interactions.

Results and Discussion

*Synthesis and spectroscopic characterization of **1** - **5**.*

The tin complexes **1-5** (Chart 1) were readily prepared by deprotonation of the parent Schiff's base ligands,[58] *N*′,*N*′-4-bis(2-hydroxybenzylidene)succinohydrazide, *N*′,*N*′-4-bis(2-hydroxybenzylidene)glutarohydrazide, or *N*′,*N*′-4-bis(2-hydroxybenzylidene)adipohydrazide, followed by the addition of R_2SnCl_2 (R = Me, Ph) in toluene. The compounds are soluble in organic solvents and can be readily separated from byproducts. Infrared and multinuclear NMR

spectroscopy support the formulation. In the infrared spectrum the ν(C=N) stretch shifts to lower wavenumbers (1606-1608 cm^{-1}) compared to the free ligand (1621 cm^{-1}) and new bands appear at 400-600 cm^{-1} which may be assigned to ν(Sn—O) and ν(Sn—N).[59,60] The presence of tin satellites on the imino proton in the ^{1}H NMR spectrum and phenolate aromatic carbon in the $^{13}C\{^{1}H\}$ NMR spectra confirms the binding of tin. Finally the ^{119}Sn NMR spectra shows one significantly shifted peak compared to the starting materials (**1-3**: δ_{119Sn} = -153 ppm, Me_2SnCl_2 δ_{119Sn} = +31 ppm; **4-5**: δ_{119Sn} = -331 ppm, Ph_2SnCl_2 δ_{119Sn} = -27 ppm), which is indicative of an increase in coordination number.

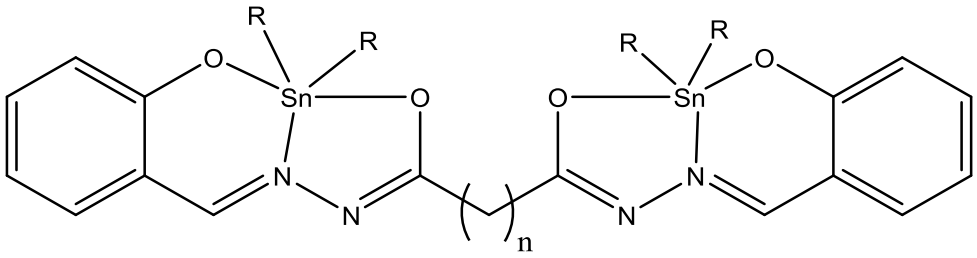

1 R = Me, n = 2;
2 R = Me, n = 3;
3 R = Me, n = 4;
4 R = Ph, n = 3;
5 R = Ph, n = 4;

Chart 1. Structures of complexes described in this work.

*Structural studies of **1-5**.*

Compounds **1-5** were additionally characterized by single crystal X-ray diffraction. The molecular structures are shown in Figures 1 and 2 and selected bond lengths for **1** are given in Table 1. The metric parameters for **2-5** are essentially the same and collated in Table S1.

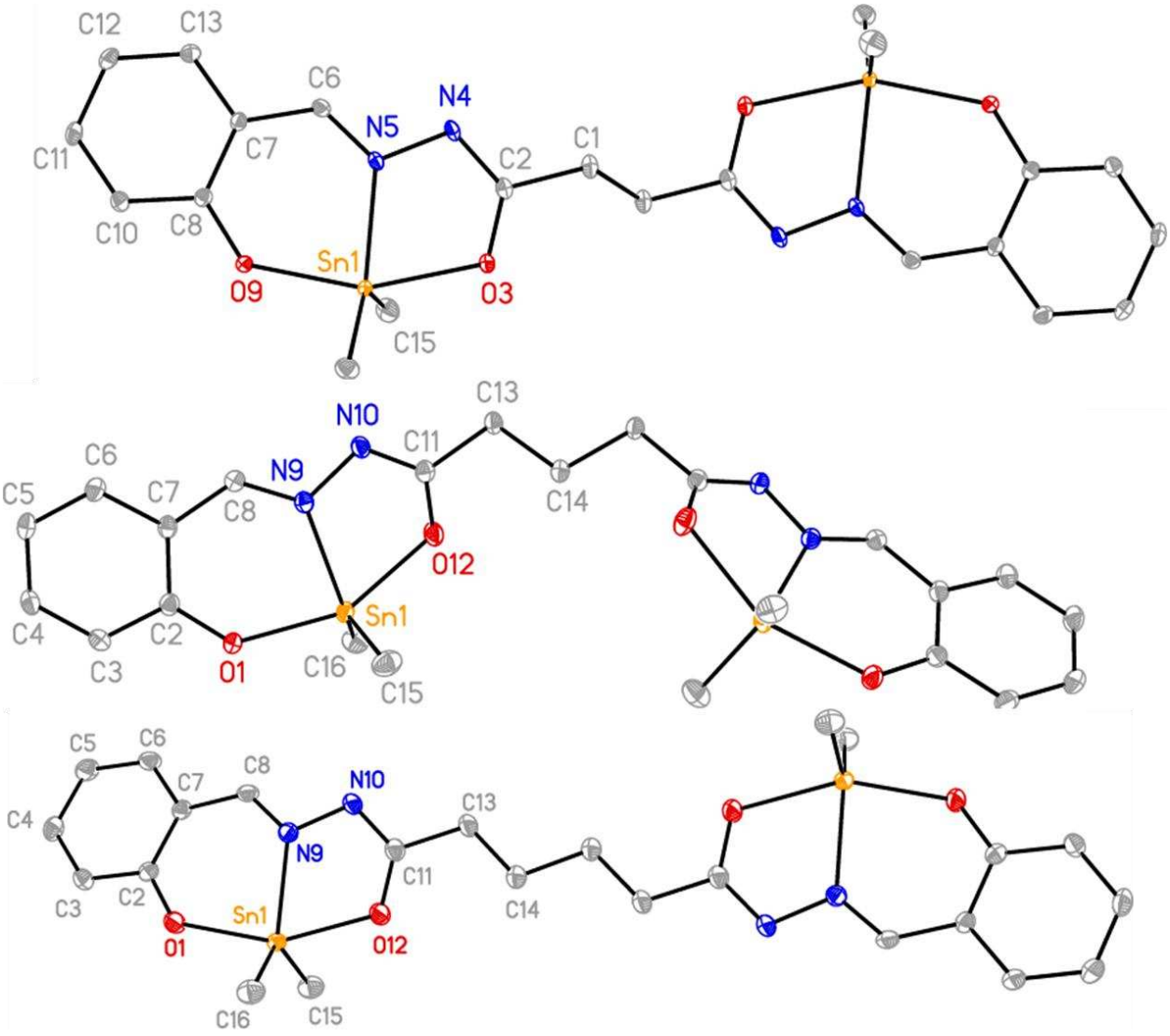

Figure 1. Molecular structures of **1** (top), **2** (middle) and **3** (bottom). Only symmetry unique atoms labelled (**1**: 1-x, -y, 1-z; **2**: 3/2-x, y, 1/2-z; **3**: 2-x, 1-y, 1-z). Atomic displacement shown at 50% probability and hydrogens omitted for clarity.

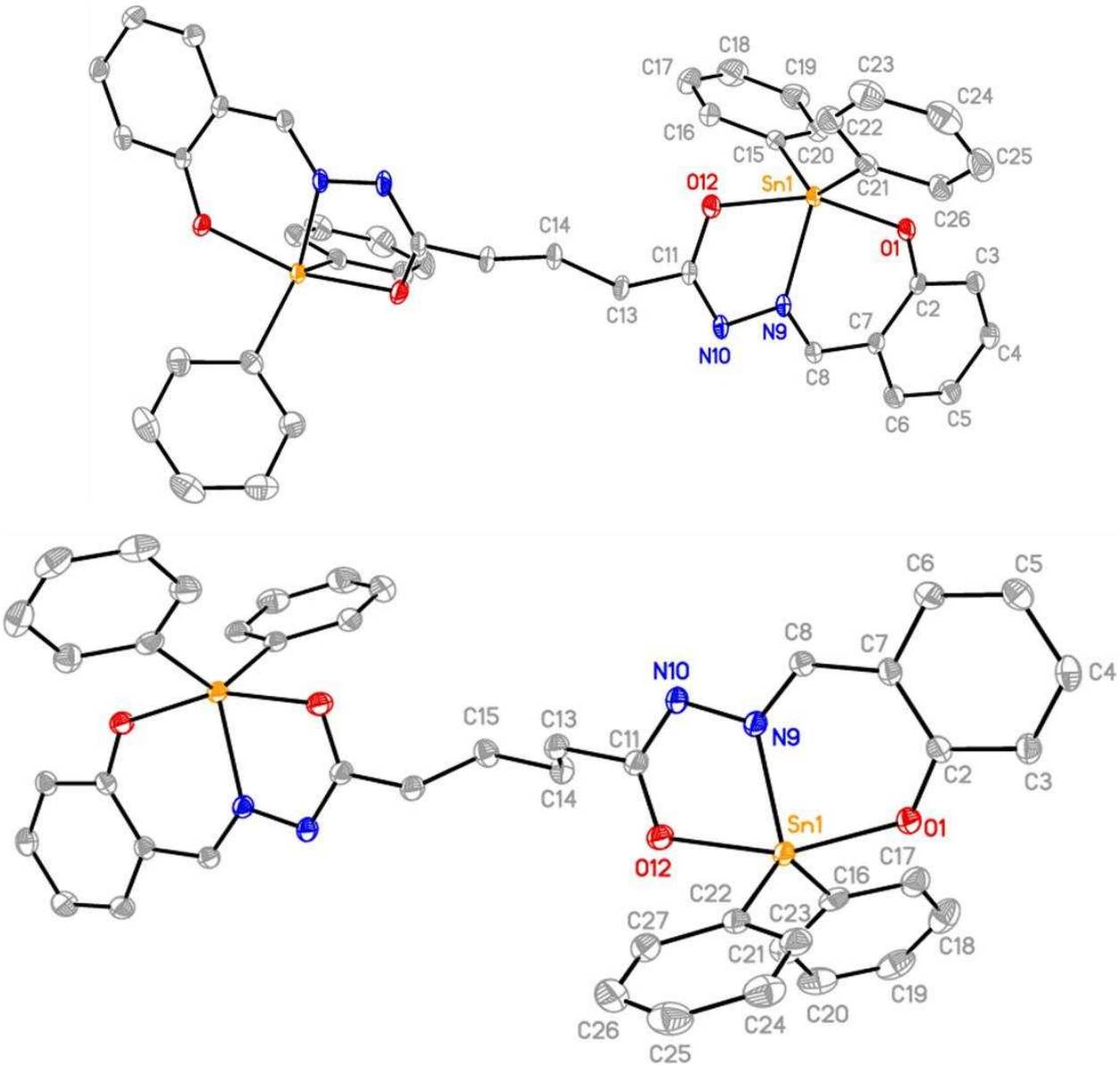

Figure 2. Symmetry generated molecule of **4** (top) and **5** (bottom), this showing one conformation of the 50% occupancy disordered butyl linking chain (C14, C15). Atomic displacement shown at 50% probability and only symmetry unique atoms labelled (**4:** 2-x, y, 3/2-z; **5**: 2-x, -y, 2-z). Hydrogen atoms omitted for clarity.

In the structure of **1**, the tin atom is in a distorted trigonal bipyramidal environment where the nitrogen and methyl groups are the trigonal plane and the oxygen groups are axial, where the O—Sn—O angle is 155.33(5)°. Inspection of the space-filling diagram (Figure 3) shows that the tin atom is not coordinatively saturated by the ligand; calculations of the percent buried volume[61] taken from the structures show little change across the series **1-3** (free volume for **1** = 25.1%, **2** = 22.7%, **3** = 25.0%). The methylene spacer group does not influence the metric parameters but there is a difference in the non-covalent interactions. There is a short Sn···O intramolecular contact of 3.480(2) Å in **1** (Figure 3) and 3.456(1) Å in **2**, which are considerably shorter than the sum of the van der Waals radii (3.92 Å),[62] and form a 1D chain along the [101] direction. The two interacting molecules are coplanar, but slightly offset with the O···Sn-N(9) angle in **1** and the O···Sn-N(5) angle in **2** both identical at 154.33(4)°. There is also a short Sn···H—C_{sp2} intermolecular interaction from H(10) ($d_{C...Sn}$ = 4.089(2)Å; ∠C-H…Sn = 137.4°). In **3-5**, these interactions are no longer present. For **4** and **5** the larger phenyl groups could be a reason why these interactions are not present, but the space filling diagram (Figure 4) does not support this simple assignment; the percent buried volume calculations show a smaller free volume (**4** = 16.7%, **5** = 17.5%). The packing is now dominated by O···H—C_{sp2} weak hydrogen bonds (**4**: $d_{C...O}$ = 3.441(2) Å; **5**: $d_{C...O}$ = 3.624(3) Å) and this interaction is also present in **3** ($d_{C...O}$ = 3.465(4) Å) along with shorter N···H—C_{sp2} interactions ($d_{C...N}$ = 3.405(4) Å) from the Sn-Me group to N(10). In **3** the more flexible linker may be the reason for the lack of Sn···O interaction. These results suggest that the Sn···O interaction can perhaps compete with the C—H···O or C—H···N weak hydrogen bonds. It is also noteworthy that close inspection of the ^{1}H NMR spectra reveal no tin satellite peaks at the interacting protons, which demonstrates that these interactions do not persist in solution.

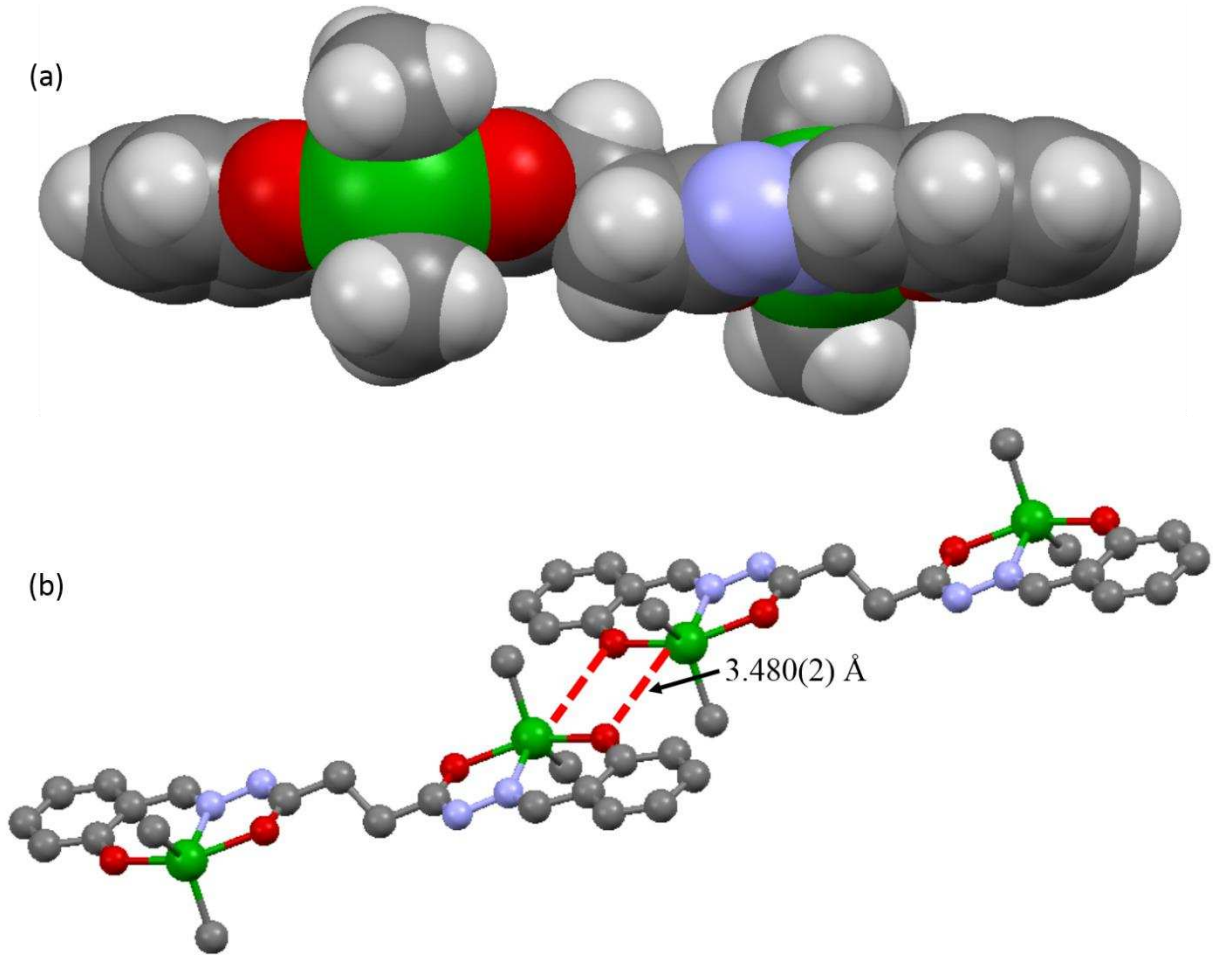

Figure 3. (a) Space filling diagram of **1**; (b) dimerization of **1** via Sn···O tetrel interactions (dashed lines).

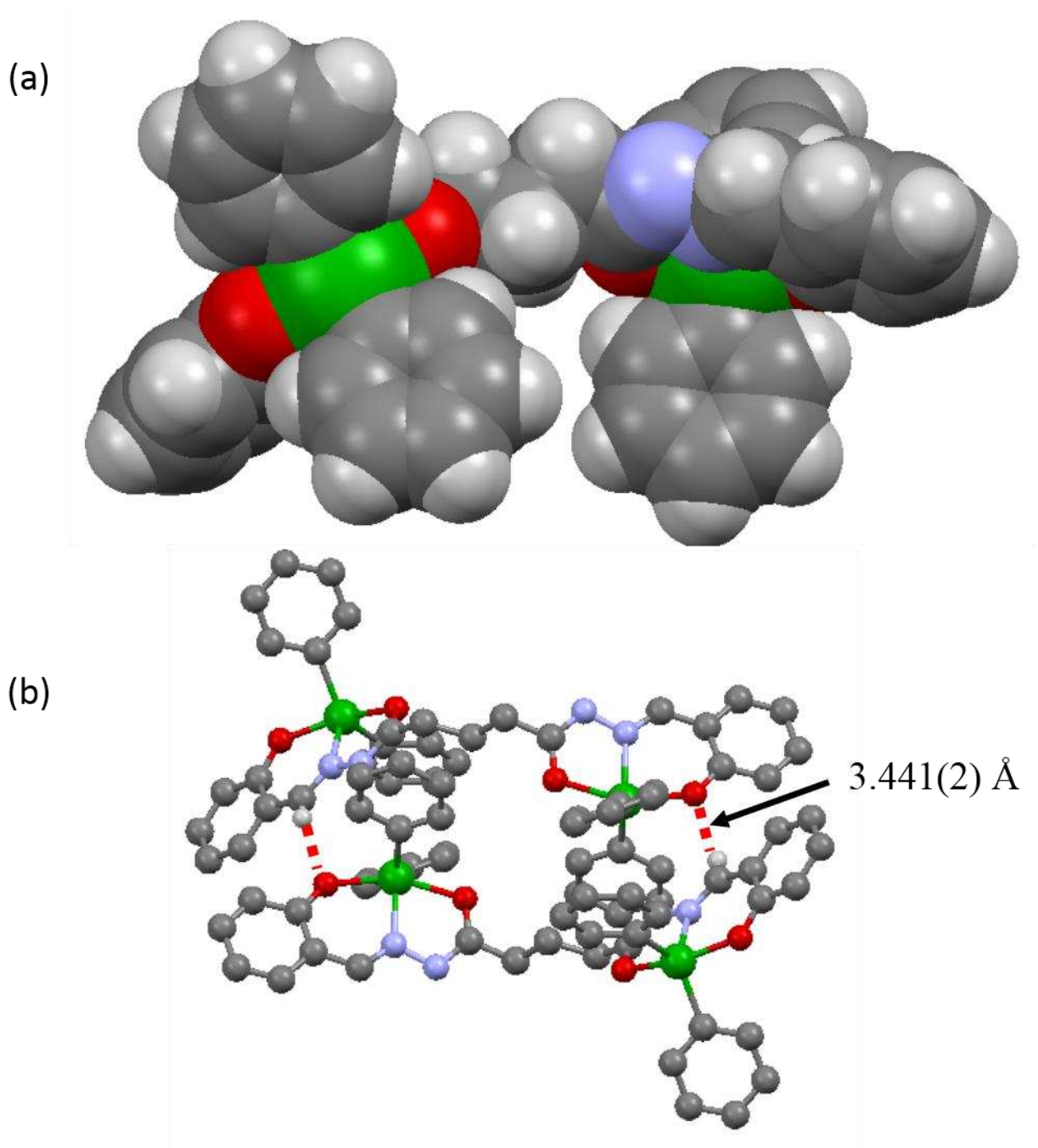

Figure 4. (a) Space filling diagram of **4**; (b) dimerization of **4** via O···H—C weak hydrogen bonds (dashed lines).

Table 1. Selected metric parameters for **1** (structural data) and **1'** (computational data).

Compound	Sn—O phenolate	Sn—O carboxylate	Sn—N	Sn—C	N—N	C=N	C—Sn—C
1	2.092(1)	2.156(2)	2.178(2)	2.114(2) 2.116(2)	1.405(2)	1.310(2) 1.294(2)	131.42(7)
1' B97-D	2.145	2.206	2.231	2.159	1.379	1.325	137.0
1' M06-2X	2.110	2.154	2.206	2.121	1.385	1.305	137.5

*Computational studies on **1**.*

In order to further characterize the Sn···O interactions we examined them via computational methods on a model system, denoted **1'**, that retains just one Sn center obtained from the crystal structure of **1** truncated at the central C—C bond. As shown in Table 1, metric parameters of Sn—O, Sn—N and Sn—C bonds are well reproduced by this approach, with slightly better agreement obtained using M06-2X verses B97-D level. The molecular electrostatic potential of **1'** projected onto an 0.001 au electron density isosurface is shown in Figure 5, and reveals a small but clear area of positive potential (+ 0.04 au) on Sn between methyl groups, as well as negative areas associated with O and N centers. Geometry optimization of a dimer of **1'** retains the relatively close Sn···O contacts, with optimal values of 3.117 Å (3.199 Å) at the M06-2X (B97-D) level notably smaller than the experimentally observed value. The excellent agreement for intramolecular geometry noted above suggests that use of **1'** as a model of **1** is not the cause of this contraction, and it may be that this results from extracting a dimer from the crystalline environment (hence removing competing interactions). In any case, DFT predictions concur with experiment

that close Sn···O contacts are indeed possible. Finally, the total interaction energy of the dimer **1'** is -67.03 kJ/mol (B97-D level of theory).

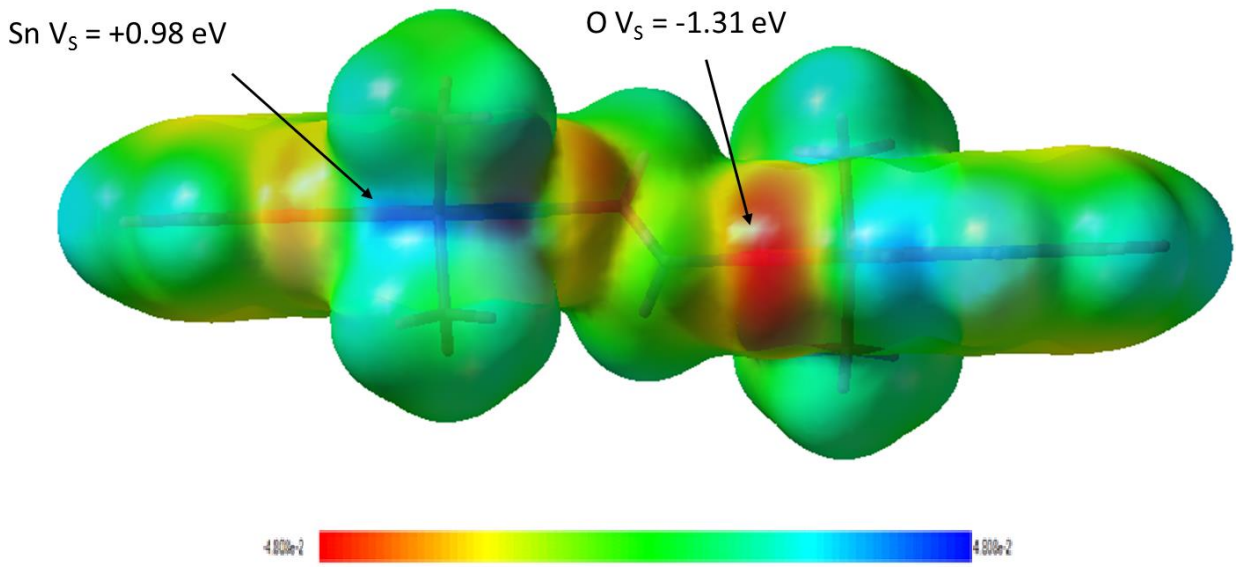

Figure 5. Molecular electrostatic potential of **1'** dimer mapped onto 0.001 au electron density isosurface.

Atoms-in-Molecules (AIM) analysis of the M06-2X electron density results in bond paths corresponding to intermolecular Sn···O interactions, as well as paths for C—H···O, C—H···Sn and H···H contacts, as shown in Figure 6. The value of the electron density at the corresponding bond critical point (ρ_c) is widely used as a measure of the strength of non-covalent interactions, with values reported in Table 2 that are similar to those reported in the literature for tetrel bonding.[46,63,64] These show that the Sn···O contact is comparable with C—H···O, with weaker C—H···Sn and H···H contacts. All bond critical points have positive Laplacian ($\nabla^2\rho_c$) and zero or slightly positive

energy density (H_c), and so seem best described as weak electrostatic contacts with little or no covalent character.

Table 2. Bond critical point data for intermolecular contacts (au).

	Number	ρ_c	$\nabla^2\rho_c$	H_c
Sn···O	2	0.011	+0.033	+0.001
C—H···O	4	0.010	+0.039	+0.001
C—H···Sn	2	0.007	+0.020	0.000
H···H	2	0.005	+0.017	0.000

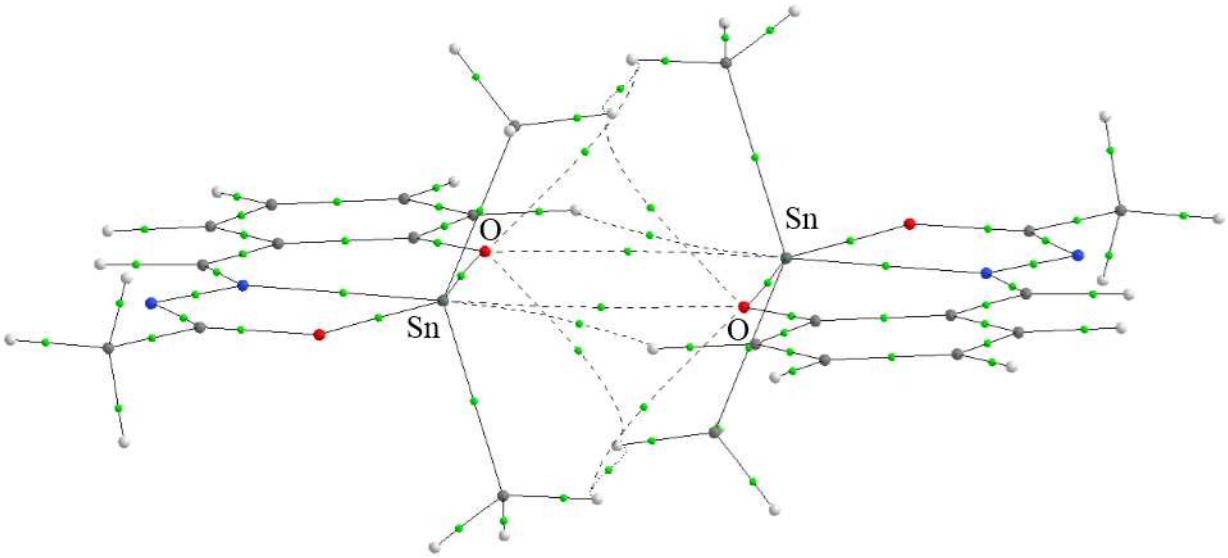

Figure 6. Molecular graph of **1'** dimer: bond critical points are represented by green dots, intramolecular bond paths by solid lines, and intermolecular bond paths by dotted lines. Only atoms involved in tetrel bonding labeled.

Conclusion

In conclusion we have isolated and structurally characterized two examples of compounds that feature short non-covalent interactions between a tin atom and an oxygen atom that are well within the van der Waals radii of the two atoms. However these are not present when the methyl groups are replaced by phenyl groups or when the linker between the two Schiff base fragments is lengthened. DFT and AIM methodologies show that this interaction has comparable strength to C—H···O interactions, but is principally electrostatic in origin.

Experimental

^{1}H, $^{13}C\{^{1}H\}$ and ^{119}Sn NMR spectra were recorded on a Bruker AV400 spectrometer operating at 400.23 MHz, 155.54 MHz and 149.2 MHz respectively, and were referenced to the residual ^{1}H and ^{13}C resonances of the solvent used and external $SnMe_4$. Numbering of the spectra is shown in Figure 7 and assignments were verified using 2D experiments. IR spectra were recorded on a Bruker Tensor II spectrometer with attenuated total reflectance (ATR) accessory. Mass spectra were measured on a MALDI QTOF Premier MS system. X-ray crystallography data were measured on a Bruker D8 Quest Eco with an Oxford Cryostream at 100 K. Using Olex2, the structures were solved with the XT structure solution program using Intrinsic Phasing and refined with the XL refinement package using Least Squares minimization.[65,66,67] Crystal data, details of data collections and refinement are given in Table 3. The ligands were made via literature procedures.[58] All chemicals and solvents were obtained from commercial sources and used as received.

DFT calculations were carried out in Gaussian09[68] with the meta-hybrid M06-2X and dispersion corrected B97D functionals[69,70] and def2-TZVP basis set[71] used in previous work, and taking advantage of density fitting to make larger calculations viable where possible. All calculations of interaction energy used the counterpoise method to account for basis set superposition energy.[72] Converged molecular orbitals were obtained from these calculations and used for topological analysis of the resulting electron density using the AIMAll package.[73]

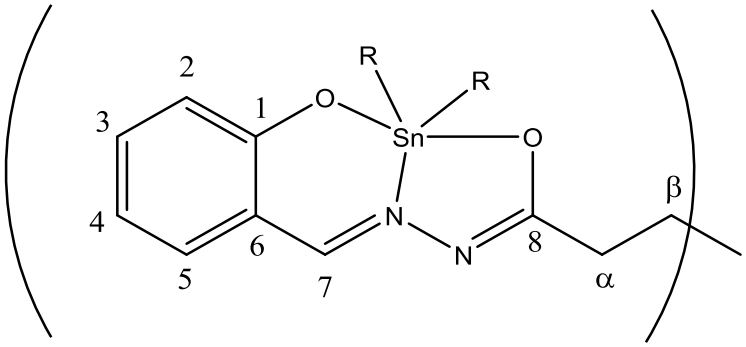

Figure 7. Numbering scheme for NMR assignments.

Synthesis of complexes 1-5

The compounds **1-5** were synthesized via the same general procedure. The ligand (0.30 g) was reacted with 4 equivalents of Et_3N in dry toluene and stirred for 30 minutes at room temperature. 2 equivalents of R_2SnCl_2 were added and the mixture refluxed for 6 hours to yield a yellow solution and a white precipitate. Filtration and removal of the solvent afforded the crude product which was recrystallized from a 3:2 vol:vol mixture of chloroform and hexane. Single crystals suitable for X-ray diffraction were obtained by slow evaporation of the solvent mixture.

1: Yield 0.20 g, 83%. M.Pt. 245-246 ºC. IR $\tilde{\nu}$ (cm^{-1}): 1608 (s, C=N), 1548 (m, C-O), 1505 (m), 1475 (m), 1445 (m), 1366 (m), 1362 (m), 1298 (s, Ar-O), 1161 (m), 996 (w, N-N), 969 (w), 903 (m), 757 (m), 602 (m, Sn-C), 563 (m), 556 (m, Sn-O), 523 (m, Sn-C), 463 (m, Sn-N), 326 (m), 320 (m). ^{1}H NMR ($CDCl_3$) δ (ppm): 0.77 (s, 12H, $^{2}J_{Sn-H}$ = 77 Hz, SnMe), 2.66 (s, 4H, α), 6.74 (t, 2H, $^{3}J_{H-H}$ = 7.4 Hz, H4), 6.76 (d, 2H, $^{3}J_{H-H}$ = 8.5 Hz, H2), 7.14 (d, 2H, $^{3}J_{H-H}$ = 7.9 Hz, H5), 7.33 (t, 2H, 7.7 Hz, H3), 8.59 (s, 2H,$^{3}J_{Sn-H}$ = 47.0 Hz, H7). $^{13}C\{^{1}H\}$ NMR ($CDCl_3$) δ (ppm): 1.3 (SnMe, $^{1}J_{Sn-C}$ = 649 Hz), 30.5 (Cα), 116.5 (C6), 117.2 (C4), 121.6 (C2), 134.2 (C5), 135.2 (C3), 161.1 (C7), 166.2 (C1), 174.6 (C8).^{119}Sn NMR ($CDCl_3$): δ -153.1. HRMS (MALDI): calculated for $C_{22}H_{26}N_4O_4Sn_2$ 649.9998, found: 650.0013 [M^+].

2: Yield 0.22 g, 83%. M.Pt. 135-136 ºC. IR ṽ (cm^{-1}): 1607 (s, C=N), 1546 (m, C-O), 1513 (m), 1472 (m), 1444 (m), 1363 (m), 1288 (s, Ar-O), 1201, 1156, 1013 (m), 999 (w, N-N), 969 (w), 902 (m), 757 (m), 606 (m, Sn-C), 559 (m, Sn-O), 517 (m, Sn-C), 459 (m, Sn-N), 403, 344, 322, 248 (m). ^{1}H NMR ($CDCl_3$) δ (ppm): 0.79 (s, 12H, $^{2}J_{Sn-H}$ = 76.9 Hz, Sn-Me), 2.03 (quint., 2H, 7.7 Hz, β), 2.39 (t, 4H, 7.3 Hz, α), 6.74 (t, 2H, $^{3}J_{H-H}$ = 7.4 Hz, H4), 6.76 (d, 2H, $^{3}J_{H-H}$ = 8.7 Hz, H2), 7.14 (d, 2H, $^{3}J_{H-H}$ = 8.0 Hz, H5), 7.34 (t, 2H, 7.6 Hz, H3), 8.60 (s, 2H,$^{3}J_{Sn-H}$ = 47 Hz, H7). $^{13}C\{^{1}H\}$ NMR ($CDCl_3$) δ (ppm): 1.3 (SnMe), 22.6 (Cβ), 33.9 (Cα), 116.5 (C6), 117.2 (C4), 121.6 (C2), 134.2 (C5), 135.2 (C3), 161.1 (C7), 166.2 (C1), 175.2 (C8). ^{119}Sn NMR ($CDCl_3$): δ -153.1. HRMS (MALDI): calculated for $C_{23}H_{29}N_4O_4Sn_2$ 665.0233, found: 665.0253 [MH^+].

3: Yield 0.25 g, 83%. M.Pt. 200-201 ºC. IR ṽ (cm^{-1}): 1606 (s, C=N), 1546 (m, C-O), 1512 (m), 1471 (m), 1446 (m), 1396, 1369, 1331 (m), 1299 (s, Ar-O), 1203, 1155 (m), 1013 (w, N-N), 903 (w), 761 (m), 605 (m, Sn-C), 561 (m, Sn-O), 523 (m, Sn-C), 458 (m, Sn-N), 425, 344, 305 (m).

^{1}H NMR ($CDCl_3$) δ (ppm): 0.79 (s, 12 H, $^{2}J_{Sn-H}$ = 77 Hz, SnMe). 1.88 (m, 4H, β), 2.35 (m, 4H, α), 6.74 (t, 2H, $^{3}J_{H-H}$ = 7.7 Hz, H4), 6.76 (d, 2H, $^{3}J_{H-H}$ = 8.2 Hz, H2), 7.14 (d, 2H, $^{3}J_{H-H}$ = 8.0 Hz, H5), 7.33 (t, 2H, $^{3}J_{H-H}$ = 7.7 Hz, H3), 8.59 (s, 2H, $^{3}J_{Sn-H}$ = 47 Hz, H7). $^{13}C\{^{1}H\}$ NMR ($CDCl_3$) δ (ppm): 1.2 (SnMe, $^{1}J_{Sn-C}$ = 647 Hz), 26.0 (Cβ), 34.2 (Cα), 116.5 (C6), 117.2 (C4), 121.6 (C2), 134.2 (C5), 135.2 (C3), 161.0 (C7), 166.2 (C1), 175.5 (C8). ^{119}Sn NMR ($CDCl_3$): δ -153.9. HRMS (MALDI): calculated for $C_{24}H_{30}N_4O_4Sn_2$ 678.0311, found: 678.0466 [M^+].

4: Yield 0.21 g, 70%. M.Pt. 215-216 ºC. IR ṽ (cm^{-1}): 1609 (s, C=N), 1545 (m, C-O), 1518 (m), 1470 (m), 1448 (m), 1430, 1365, 1300 (m), 1300 (s, Ar-O), 1204, 1156 (m), 1077 (w, N-N), 998 (w), 760, 728, 693, 571 (m, Sn-O) , 461 (m, Sn-N), 438, 334, (m), 283 (m, Sn-C), 238 (m, Sn-C). ^{1}H NMR ($CDCl_3$) δ (ppm): 2.33 (quint, 2H, $^{3}J_{H-H}$ = 8.1 Hz, β), 2.62 (t, 4H, $^{3}J_{H-H}$ = 7.6 Hz, α), 6.80 (t, 2H, $^{3}J_{H-H}$ = 7.6 Hz, H4), 7.13 (d, 2H, $^{3}J_{H-H}$ = 8.5 Hz, H2), 7.19 (d, 2H, $^{3}J_{H-H}$ = 7.9 Hz, H5), 7.43 (m, 4H, *para*-Ar), 7.44 (m, 8H, *meta*-Ar), 7.88 (m, 8H, $^{3}J_{Sn-H}$ = 79 Hz, *ortho*-Ar), 8.64 (s, 2H, $^{3}J_{Sn-H}$ = 52 Hz, H7). $^{13}C\{^{1}H\}$ NMR ($CDCl_3$) δ (ppm): 23.1 (β), 34.3 (α), 116.6 (C6), 117.5 (C4), 122.1 (C2), 128.9 ($^{3}J_{Sn-C}$ = 85 Hz, *meta*-Ar), 130.5 (*para*-Ar), 134.4 (C5), 135.4 (C3), 136.2 ($^{2}J_{Sn-C}$ = 55 Hz, *ortho*-Ar), 139.1 (*ipso*-Ar), 161.2 (C7), 167.1 (C1), 175.3 (C8). ^{119}Sn NMR ($CDCl_3$): δ -331.9. HRMS (MALDI): calculated for $C_{43}H_{37}N_4O_4Sn_2$ 913.0859, found: 913.0905 [MH^+].

5: Yield 0.25 g, 83%. M.Pt. 165-166 ºC. IR ṽ (cm^{-1}): 1608 (s, C=N), 1546 (m, C-O), 1515 (m), 1471 (m), 1447 (m), 1430, 1365 (m), 1300 (s, Ar-O), 1202, 1157 (m), 1076 (w, N-N), 997 (w), 900, 759, 730, 695, 574 (m, Sn-O), 519, 461 (m, Sn-N), 439, 425, 344, 305 (m), 353, 302, 283 (m, Sn-C), 202, 238 (m, Sn-C). ^{1}H NMR ($CDCl_3$) δ (ppm): 1.95 (m, 4H, β), 2.56 (m, 4H, α), 6.80 (t,

2H, $^{3}J_{H-H}$ = 7.4 Hz, H4), 7.12 (d, 2H, $^{3}J_{H-H}$ = 8.4 Hz, H2), 7.18 (d, 2H, $^{3}J_{H-H}$ = 7.9 Hz, H5), 7.40 (m, 4H, *para*-Ar), 7.42 (m, 8H, *meta*-Ar), 7.86 (d, 8H, $^{3}J_{Sn-H}$ = 80 Hz, $^{3}J_{H-H}$ = 7.6 Hz, *ortho*-Ar), 8.62 (s, 2H, $^{3}J_{Sn-H}$ = 52 Hz, H7). $^{13}C\{^{1}H\}$ NMR ($CDCl_3$) δ (ppm): 26.1 (β), 34.4 (α), 116.6 (C6), 117.5(C4), 122.0 (C2), 128.9 ($^{3}J_{Sn-C}$ = 87.0 Hz, *meta*-Ar), 130.5 (*para*-Ar), 134.4 (C5), 135.4 (C3), 136.2 ($^{2}J_{Sn-C}$ = 54 Hz, *ortho*-Ar), 139.1 ($^{1}J_{Sn-C}$ = 73 Hz, *ipso*-Ar), 161.0 (C7), 167.1 (C1), 175.7 (C8). ^{119}Sn NMR ($CDCl_3$): δ -331.7. HRMS (MALDI): calculated for $C_{44}H_{39}N_4O_4Sn_2$ 927.1015, found: 927.1041 [MH^+].

Table 3. Crystal Data and Refinement Parameters for Complexes **1-5.**

	1	**2**	**3**	**4**	**5**
CCDC Number	1548813	1548814	1548815	1548816	1548817
Empirical formula	$C_{22}H_{26}N_4O_4Sn_2$	$C_{23}H_{28}N_4O_4Sn_2$	$C_{24}H_{30}N_4O_4Sn_2$	$C_{43}H_{36}N_4O_4Sn_2$	$C_{44}H_{38}N_4O_4Sn_2$
Formula weight	647.85	661.87	675.90	910.14	924.16
Crystal system	Triclinic	Monoclinic	Monoclinic	Monoclinic	Monoclinic
Space Group	$P\bar{1}$	P2/n	$P2_1/c$	I2/c	$P2_1/c$
a (Å)	7.1611(3)	10.4882(3)	10.3686(4)	12.6518(5)	15.3416(6)
b (Å)	8.7695(4)	9.6493(3)	10.4987(4)	10.5353(4)	9.9387(4)
c (Å)	9.5314(4)	13.2514(4)	12.5434(5)	29.1308(11)	12.9922(5)
α (^{o})	82.4992(15)	90	90	90	90
β (^{o})	81.4935(15)	109.9250(10)	109.6852(18)	101.102(2)	103.1630(12)
γ (^{o})	80.5682(14)	90	90	90	90
V (Å^3)	580.50(4)	1260.81(7)	1285.64(9)	3810.2(3)	1928.94(13)
Z	1	2	2	4	2
Temperature (K)	100(2)	100(2)	100(2)	100(2)	100(2)
Density (calculated) (Mg/m^3)	1.853	1.743	1.746	1.587	1.591

Absorption coefficient (mm^{-1})	2.187	2.016	1.979	1.359	1.344
F(000)	318	652	668	1816	924
Crystal size	0.41 x 0.25 x 0.2	0.28 x 0.26 x 0.05	0.42 x 0.25 x 0.22	0.3 x 0.13 x 0.09	0.38 x 0.15 x 0.14
Theta range for data collection (^{o})	3.036 to 28.484	2.670 to 28.760	2.596 to 28.432	2.750 to 28.383	2.766 to 30.680
Limiting Indices	-9≤h≤9 -11≤k≤11 -12≤l≤12	-14≤h≤14 -13≤k≤13 -17≤l≤17	-13≤h≤13 -14≤k≤14 -16≤l≤16	-16≤h≤16 -12≤k≤14 -35≤l≤38	-21≤h≤21 -14≤k≤14 -18≤l≤18
Reflections collected	16099	64554	17463	35085	40101
Independent reflections	2922 [R(int) = 0.0503]	3269 [R(int) = 0.0291]	3238 [R(int) = 0.0354]	4764 [R(int) = 0.0260]	5959 [R(int) = 0.0428]
Completeness to theta (%)	99.6 %	99.7 %	100.0 %	99.7 %	99.9 %
Refinement method	Full-matrix least-squares on F^2	Full-matrix least-squares on F^2	Full-matrix least-squares on F^2	Full-matrix least-squares on F^2	Full-matrix least-squares on F^2
Data / restraints / parameters	2922 / 0 / 147	3269 / 0 / 152	3238 / 1 / 144	4764 / 0 / 240	5959 / 0 / 253
Goodness-of-fit on F^2	1.142	1.145	1.133	1.057	1.015
Final R indices [I>2σ(I)]	R_1 = 0.0181 wR_2 = 0.0472	R_1 = 0.0162 wR_2 = 0.0398	R_1 = 0.0265 wR_2 = 0.0568	R_1 = 0.0196 wR_2 = 0.0440	R_1 = 0.0261 wR_2 = 0.0529

R indices (all data)	$R_1 = 0.0189$ $wR_2 = 0.0477$	$R_1 = 0.0192$ $wR_2 = 0.0409$	$R_1 = 0.0357$ $wR_2 = 0.0615$	$R_1 = 0.0249$ $wR_2 = 0.0463$	$R_1 = 0.0468$ $wR_2 = 0.0602$
Largest diff. peak and hole ($e.Å^{-3}$)	0.413 and -1.276	0.502 and -0.416	1.103 and -1.112	0.438 and -0.598	0.798 and -0.637

ASSOCIATED CONTENT

AUTHOR INFORMATION

Corresponding Author

* Tel: +353-1-8963501. Fax: +353-1-6712826. E-mail: bakerrj@tcd.ie

ORCID ID

Robert J. Baker: 0000-0003-1416-8659

Muhammad Khawar Rauf: 0000-0001-9994-4033

Author Contributions

The manuscript was written through contributions of all authors. All authors have given approval to the final version of the manuscript.

ACKNOWLEDGMENT

HU thanks the Higher Education Commission of Pakistan. JAP is grateful to Advanced Research Computing @ Cardiff (ARCCA) for computing facilities.

Supporting Information. Full crystallographic descriptions (CIF), spectroscopic and computational details. This material is available free of charge via the Internet at http://pubs.acs.org.

References

(1) Lehn, J. -M. Supramolecular Chemistry. Concepts and Perspectives; VCH, Weinheim, Germany, 1995.

(2) Lehn, J. -M. *Angew. Chem., Int. Ed.* **1988**, *27*, 89–112.

(3) Neel, A. J.; Hilton, M. J.; Sigman, M. S.; Toste, F. D. *Nature* **2017**, *543*, 637-646.

(4) Bulfield, D.; Huber, S. M. *Chem. Eur. J.* **2016**, *22*, 14434-14450.

(5) Cavallo, G.; Metrangolo, P.; Milani, R.; Pilati, T.; Priimagi, A.; Resnati, G.; Terraneo, G. *Chem. Rev.* 2016, **116,** 2478-–2601.

(6) Bauzá, A.; Mooibroek, T. J.; Frontera, A. *ChemPhysChem* **2015**, *16*, 2496-2517.

(7) Gilday, L. C.; Robinson, S. W.; Barendt, T. A.; Langton, M. J.; Mullaney, B. R.; Beer, P. D. *Chem. Rev*. **2015**, *115*, 7118-7195.

(8) Troff, R. W.; Makela, T.; Topic, F.; Valkonen, A.; Raatikainen, K.; Rissanen, K. *Eur. J. Org. Chem.* **2013**, 1617-1637.

(9) Wang, H.; Wang, W.; Jin, W. J. *Chem. Rev.* **2016***, 116,* 5072–5104.

(10) Kolář, M. H.; Hobza P. *Chem. Rev.* **2016,** *116*, 5155–5187.

(11) Sure, R.; Grimme, S., *Chem. Commum.* **2016**, *52*, 9893-9896.

(12) Politzer, P.; Murray, J. S.; Clark, T. *Phys. Chem. Chem. Phys*. **2013**, *15*, 11178-11189.

(13) Politzer, P.; Murray, J. S. *ChemPhysChem* **2013**, *14*, 278-294.

(14) Politzer, P.; Murray, J. S.; Clark, T. *Phys. Chem. Chem. Phys.* **2010**, *12*, 7748-7757.

(15) Bauzá, A.; Mooibroek T. J.; Frontera, A. *The Chemical Record*, **2016**, *16*, 473–487.

(16) Grabowski, S. J. *Phys. Chem. Chem. Phys.* **2014**, *16*, 1824-1834.

(17) Bauzá, A.; Ramis, R.; Frontera, A. *Comput. Theor. Chem.* **2014**, *1038*, 67-70.

(18) Bauzá, A.; Mooibroek, T. J.; Frontera, A. *Chem. Eur. J.* **2014**, *20*, 10245-10248.

(19) Bauzá, A.; Mooibroek, T. J.; Frontera, A. *Angew. Chem. Int. Edn.* **2013**, *52*, 12317-12321.

(20) Del Bene, J. E.; Alkorta, I.; Elguero, J. *Noncovalent Forces: Challenges and Advances in Computational Chemistry and Physics*, ed. Scheiner, S. Springer: New York, **2015**, *19*, 191–263.

(21) Setiawan, D.; Kraka, E.; Cremer, D. *J. Phys. Chem. A* **2015**, *119*, 1642–1656.

(22) Sarkar, S.; Pavan, M. S.; Guru Row, T. N. *Phys. Chem. Chem. Phys.* **2015**, *17*, 2330–2334.

(23) Guan, L.; Mo, Y. *J. Phys. Chem. A* **2014**, *118*, 8911–8921.

(24) Del Bene, J. E.; Alkorta, I.; Elguero, J. *J. Phys. Chem. A* **2014**, *118*, 3386–3392.

(25) Politzer, P.; Murray, J. S.; Janjić, G. V.; Zarić, S. D. *Crystals* **2014**, *4*, 12–31.

(26) Eskandri, K.; Mahmoodabadi, N. *J. Phys. Chem. A* **2013**, *117*, 13018–13024.

(27) Scheiner, S. *Acc. Chem. Res.* **2013**, *46*, 280–288.

(28) Scheiner, S. *Int. J. Quantum Chem.* **2013**, *113*, 1609–1620.

(29) Adhikary, U.; Scheiner, S. *J. Chem. Phys.* **2011**, *135*, 184306.

(30) Zahn, S.; Frank, R.; Hey-Hawkins, E.; Kirchner, B. *Chem. – Eur. J.* **2011**, *17*, 6034–6038.

(31) Kilian, P.; Slawin, A. M. Z.; Woollins, J. D.; *Chem. – Eur. J.* **2003**, *9*, 215–222.

(32) Shukla, R.; Chopra, D. *Phys. Chem. Chem. Phys.* **2016**, *18*, 13820-13829.

(33) Pang, X.; Jin, W. J. *New J. Chem.* **2015**, *39*, 5477−5483.

(34) Azofra, L. M.; Alkorta, I.; Scheiner, S. *J. Phys. Chem. A* **2015**, *119*, 535−541.

(35) Si, M. K.; Lo, R.; Ganguly, B. *Chem. Phys. Lett.* **2015**, *631−632*, 6−11.

(36) Esrafili, M.; Mohammadian-Sabet, F. *Struct. Chem.* **2015**, *26*, 199−206.

(37) Nziko, V. d. P. N.; Scheiner, S. *J. Org. Chem.* **2015**, *80*, 2356−2363.

(38) Garrett, G. E.; Gibson, G. L.; Straus, R. N.; Seferos, D. S.; Taylor, M. S. *J. Am. Chem. Soc.* **2015**, *137*, 4126–4133.

(39) Thomas, S. P.; Satheeshkumar, K.; Mugesh, G.; Guru Row, T. N. *Chem. – Eur. J.* **2015**, *21*, 6793–6800.

(40) Shukla, R.; Chopra, D. *J. Phys. Chem. B* **2015**, *119*, 14857–14870.

(41) Adhikari, U.; Scheiner, S. *J. Phys. Chem. A* **2014**, *118*, 3183−3192.

(42) Tsuzuki, S.; Sato, N. *J. Phys. Chem. B* **2013**, *117*, 6849–6855.

(43) Murray, J. S.; Lane, P.; Politzer, P. *Int. J. Quantum Chem.* **2008**, *108*, 2770–2781.

(44) Wang, W.; Ji, B.; Zhang, Y. *J. Phys. Chem. A* **2009**, *113*, 8132–8135.

(45) Bauzá, A.; Frontera, A. *Angew. Chem. Int. Ed.* **2015**, *54*, 7340-7343.

(46) Grabowski, S. J.; Sokalski, W. A. *ChemPhysChem* **2017**, DOI: 10.1002/cphc.201700224.

(47) Bauzá, A.; Mooibroek, T. J.; Frontera, A. *ChemPhysChem* **2015**, *16*, 2496-2517.

(48) Southern, S. A.; Errulat, D.; Frost, J.; Gabidullin, B.; Bryce, D. L., *Faraday Discus.* **2017**, DOI: 10.1039/C7FD00087A

(49) Mahmoudi, G.; Bauzá, A.; Amini, M.; Molins, E.; Mague, J. T.; Frontera, A. *Dalton Trans.* **2016**, *45*, 10708-10716.

(50) Servati Gargari, M.; Stilinović, V.; Bauzá, A.; Frontera, A.; McArdle, P.; Van Derveer, D.; Ng, S. W.; Mahmoudi, G. *Chem. Eur. J.* **2015**, *21*, 17951-17958.

(51) Thomas, S. P.; Pavan, M. S.; Guru Row, T. N. *Chem. Commun.* **2014**, *50*, 49-51.

(52) Mani, D.; Arunan, E. *Phys. Chem. Chem. Phys.* **2013**, *15*, 14377-14383.

(53) Sohail, M.; Panisch, R.; Bowden, A.; Bassindale, A. R.; Taylor, P. G.; Korlyukov, A. A.; Arkhipov, D. E.; Male, L.; Callear, S.; Coles, S. J.; Hursthouse, M. B.; Harrington, R. W., Clegg, W. *Dalton. Trans.* **2013**, *42*, 10971-10981.

(54) Mikosch, J.; Trippel, S.; Eichhorn, C.; Otto, R.; Lourderaj, U.; Zhang, J. X.; Hase, W.L.; Weidemüller, M.; Wester, R., *Science* **2008**, *319*, 183-186.

(55) Langer, J.; Matejcik, S.; Illenberger, *Phys. Chem. Chem. Phys.* **2000**, *2*, 1001-1005.

(56) Levy, C. J.; Puddephatt, R. J. *J. Am. Chem. Soc.* **1997**, *119*, 10127-10136.

(57) See: Grabowski, S. J. *Appl. Organomet. Chem.* **2017**, DOI: 10.1002/aoc.3727.

(58) Ranford, J. D.; Vittal, J. J.; Wang, Y. M. *Inorg. Chem.* **1998**, *37*, 1226-1231.

(59) Yearwood, B.; Parkin, S.; Atwood, D. A. *Inorg. Chim. Acta* **2002**, *333*, 124-131.

(60) Sedaghat, T.; Naseh, M.; Khavasi, H. R.; Motamedi, H. *Polyhedron* **2012**, *33*, 435-440.

(61)Falivene, L.; Credendino, R.; Poater, A.; Petta, A.;Serra, L.; Oliva, R.; Scarano, V.; Cav allo, L. *Organometallics*, **2016**, *35*, 2286-2293.

(62) Alvarez, S. *Dalton Trans.* **2013**, *42*, 8617-8636.

(63) Yourdkhani, S.; Korona, T.; Hadipour, N. L. *J Comput. Chem.* **2015**, *36*, 2412-2428.

(64) Liu, M.; Li, Q.; Cheng, J.; Li, W.; Li, H. –B. *J. Chem. Phys.* **2016**, *145*, 224310.

(65) Dolomanov, O.V., Bourhis, L.J., Gildea, R.J, Howard, J.A.K. & Puschmann, H., *J. Appl. Cryst.* **2009**, *42*, 339-341.

(66) Sheldrick, G.M. *Acta Cryst.* **2015**, *A71*, 3-8.

(67) Sheldrick, G.M. *Acta Cryst*. **2008**, *A64*, 112-122.

(68) Gaussian 09, Revision C.01, M. J. Frisch, G. W. Trucks, H. B. Schlegel, G. E. Scuseria, M. A. Robb, J. R. Cheeseman, G. Scalmani, V. Barone, B. Mennucci, G. A. Petersson, H. Nakatsuji, M. Caricato, X. Li, H. P. Hratchian, A. F. Izmaylov, J. Bloino, G. Zheng, J. L. Sonnenberg, M. Hada, M. Ehara, K. Toyota, R. Fukuda, J. Hasegawa, M. Ishida, T. Nakajima, Y. Honda, O. Kitao, H. Nakai, T. Vreven, J. A. Montgomery, Jr., J. E. Peralta, F. Ogliaro, M. Bearpark, J. J. Heyd, E. Brothers, K. N. Kudin, V. N. Staroverov, T. Keith, R. Kobayashi, J. Normand, K. Raghavachari, A. Rendell, J. C. Burant, S. S. Iyengar, J. Tomasi, M. Cossi, N. Rega, J. M. Millam, M. Klene, J. E. Knox, J. B. Cross, V. Bakken, C. Adamo, J. Jaramillo, R. Gomperts, R. E. Stratmann, O. Yazyev, A. J. Austin, R. Cammi, C. Pomelli, J. W. Ochterski, R. L. Martin, K. Morokuma, V. G. Zakrzewski, G. A. Voth, P. Salvador, J. J. Dannenberg, S. Dapprich, A. D. Daniels, O. Farkas, J. B. Foresman, J. V. Ortiz, J. Cioslowski, and D. J. Fox, Gaussian, Inc., Wallingford CT, **2010**.

(69) Zhao Y.; Truhlar, D. G. *Theor. Chem. Acc*. **2008**, 120, 215-241.

(70) Grimme, S. *J. Comp. Chem.* **2006**, *27*, 1787-1799.

(71) Weigend, F.; Ahlrichs, R. *Phys. Chem. Chem. Phys.* **2005**, *7*, 3297-3305.

(72) Boys, S. F.; Bernardi, F. *Mol. Phys.* **1970**, *19*, 553-566.

(73) AIMAll (Version 12.06.03), Todd A. Keith, TK Gristmill Software, Overland Park KS, USA, **2012**.

For ToC use only

Tin…Oxygen Tetrel Bonding: A Combined Structural, Spectroscopic and Computational Study

Hussain Ullah, Brendan Twamley, Amir Waseem,* Muhammed Khawar Rauf, Muhammad Nawaz Tahir, James A. Platts, and Robert J. Baker*

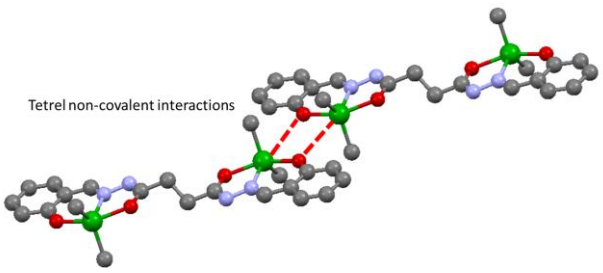

Sn…O contacts shorter than the van der Waals radii are observed in some Schiff base complexes of pentavalent tin. Computational investigation shows these are mainly electrostatic in origin.